AMERICAN SOCIETY FOR MICROBIOLOGY | mSphere®

RESEARCH ARTICLE
Host-Microbe Biology

Rousette Bat Dendritic Cells Overcome Marburg Virus-Mediated Antiviral Responses by Upregulation of Interferon-Related Genes While Downregulating Proinflammatory Disease Mediators

Joseph Prescott,[a,b] Jonathan C. Guito,[b] Jessica R. Spengler,[b] Catherine E. Arnold,[c] Amy J. Schuh,[b] Brian R. Amman,[b] Tara K. Sealy,[b] Lisa W. Guerrero,[b] Gustavo F. Palacios,[d] Mariano Sanchez-Lockhart,[d,e] Cesar G. Albariño,[b] Jonathan S. Towner[b]

[a]Center for Biological Threats and Special Pathogens, Robert Koch Institute, Berlin, Germany
[b]Viral Special Pathogens Branch, Centers for Disease Control and Prevention, Atlanta, Georgia, USA
[c]Diagnostic Systems Division, U.S. Army Medical Research Institute of Infectious Diseases, Fort Detrick, Maryland, USA
[d]Center for Genome Sciences, U.S. Army Medical Research Institute of Infectious Diseases, Fort Detrick, Maryland, USA
[e]Department of Pathology and Microbiology, University of Nebraska Medical Center, Omaha, Nebraska, USA

ABSTRACT Dysregulated and maladaptive immune responses are at the forefront of human diseases caused by infection with zoonotic viral hemorrhagic fever viruses. Elucidating mechanisms of how the natural animal reservoirs of these viruses coexist with these agents without overt disease, while permitting sufficient replication to allow for transmission and maintenance in a population, is important for understanding the viral ecology and spillover to humans. The Egyptian rousette bat (ERB) has been identified as a reservoir for Marburg virus (MARV), a filovirus and the etiological agent of the highly lethal Marburg virus disease. Little is known regarding how these bats immunologically respond to MARV infection. In humans, macrophages and dendritic cells (DCs) are primary targets of infection, and their dysregulation is thought to play a central role in filovirus diseases, by disturbing their normal functions as innate sensors and adaptive immune response facilitators while serving as amplification and dissemination agents for the virus. The infection status and responses to MARV in bat myeloid-lineage cells are uncharacterized and likely represent an important modulator of the bat's immune response to MARV infection. Here, we generate DCs from the bone marrow of rousette bats. Infection with a bat isolate of MARV resulted in a low level of transcription in these cells and significantly downregulated DC maturation and adaptive immune-stimulatory pathways while simultaneously upregulating interferon-related pathogen-sensing pathways. This study provides a first insight into how the bat immune response is directed toward preventing aberrant inflammatory responses while mounting an antiviral response to defend against MARV infection.

IMPORTANCE Marburg viruses (MARVs) cause severe human disease resulting from aberrant immune responses. Dendritic cells (DCs) are primary targets of infection and are dysregulated by MARV. Dysregulation of DCs facilitates MARV replication and virus dissemination and influences downstream immune responses that result in immunopathology. Egyptian rousette bats (ERBs) are natural reservoirs of MARV, and infection results in virus replication and shedding, with asymptomatic control of the virus within weeks. The mechanisms that bats employ to appropriately respond to infection while avoiding disease are unknown. Because DC infection and modulation are important early events in human disease, we measured the transcriptional responses of ERB DCs to MARV. The significance of this work is in identifying cell type-specific coevolved responses between ERBs and MARV, which gives insight into how

Citation Prescott J, Guito JC, Spengler JR, Arnold CE, Schuh AJ, Amman BR, Sealy TK, Guerrero LW, Palacios GF, Sanchez-Lockhart M, Albariño CG, Towner JS. 2019. Rousette bat dendritic cells overcome Marburg virus-mediated antiviral responses by upregulation of interferon-related genes while downregulating proinflammatory disease mediators. mSphere 4:e00728-19. https://doi.org/10.1128/mSphere.00728-19.

Editor W. Paul Duprex, University of Pittsburgh School of Medicine

This is a work of the U.S. Government and is not subject to copyright protection in the United States. Foreign copyrights may apply.

Address correspondence to Joseph Prescott, prescottj@rki.de, or Jonathan S. Towner, jit8@cdc.gov.

Received 4 October 2019
Accepted 12 November 2019
Published 4 December 2019

Downloaded from http://msphere.asm.org/ on April 6, 2020 by guest

bat reservoirs are able to harbor MARV and permit viral replication, allowing transmission and maintenance in the population while simultaneously preventing immunopathogenesis.

KEYWORDS Ebola virus, Marburg virus, immune response, rousette bat, viral hemorrhagic fever, virology

Egyptian rousette bats (ERBs) (*Rousettus aegyptiacus*) have been identified as a natural reservoir of Marburg virus (MARV) and Ravn virus (RAVV), collectively called marburgviruses. Furthermore, there is increasing evidence that ebolaviruses, including Ebola virus (EBOV), also in the family *Filoviridae*, are hosted by various species of bats (1–5). These filoviruses have caused numerous outbreaks across Africa, including the 2013–2016 Western African EBOV outbreak that resulted in over 11,000 deaths (6, 7). Following the discovery of MARV in 1967, almost 500 cases of MARV disease (MVD) have been recorded, with an overall case fatality rate of 80%. Since 2007, all outbreaks of MVD have occurred in Uganda, where ecological studies designed to identify the origin of human cases consistently pinpointed the ERB as a reservoir based on the repeated isolation of genetically diverse MARVs and RAVVs directly from ERBs (3, 8).

The human disease caused by pathogenic filoviruses is complex and involves multiple physiological pathways that ultimately result in coagulopathy and fluid leakage (9). Far more is known regarding EBOV disease (EVD) than MVD; however, the pathogenic processes are likely similar between the two virus genera (10). Central to filovirus disease is dysregulation of the immune system. These viruses target and replicate in dendritic cells (DCs) and monocytes/macrophages (9). DCs are the most important antigen-presenting cells and are central to innate immunity as well as directing subsequent adaptive immune responses (11). Upon sensing microbes, DCs simultaneously mature and traffic to secondary lymph tissue and stimulate T cells (12). The interaction of DCs and cells of the adaptive immune system dictates the quality and magnitude of the immune response generated. Human monocyte-derived DCs (MDDCs) fail to secrete cytokines and display an impaired maturation and activation phenotype in response to MARV infection (13), and interferon (IFN)-related antiviral responses are actively antagonized by viral proteins (14). Conversely, monocytes and macrophages, which are also permissive for infection, respond to MARV by strong upregulation of proinflammatory signals and mediators of vascular permeability (15, 16). It has also been hypothesized that infection of these cell types facilitates the dissemination of filoviruses upon trafficking to secondary lymph tissues and that cytolytic infection releases virions into the lymphatics (17).

Little is known about how the bat reservoirs of filoviruses respond either innately or adaptively to filovirus infection. Antibody responses are generated, showing that filoviral proteins are recognized, and antigen-presenting cells are enlisted in the response to infection (9). The roles and responses to infection of myeloid-lineage cells, such as macrophages and DCs, in rousette bats infected with MARV are unknown but are surely important for detecting MARV at the sites of infection and orchestrating the ensuing adaptive immune response. Since ERBs respond to and clear MARV infection with only mild transient liver pathology (18), we sought to determine the infection status and host response to MARV infection of ERB myeloid-derived DCs infected *in vitro* with a bat isolate of MARV. We found that ERB DCs support low-level MARV replication and that MARV-infected DCs transcribe steady-state levels of viral RNA (vRNA). MARV infection induced host gene transcriptional changes in ERB DCs disparate from what is observed in humans. There was a strong and sustained upregulation of type I IFN-related antiviral genes. Conversely, DC maturation genes and proinflammatory responses were downregulated upon infection, consistent with a hypothesized immune tolerance model of MARV infection control by ERBs (19). This response to MARV infection in specialized innate immune cells of the natural reservoir suggests the

Downloaded from http://msphere.asm.org/ on April 6, 2020 by guest

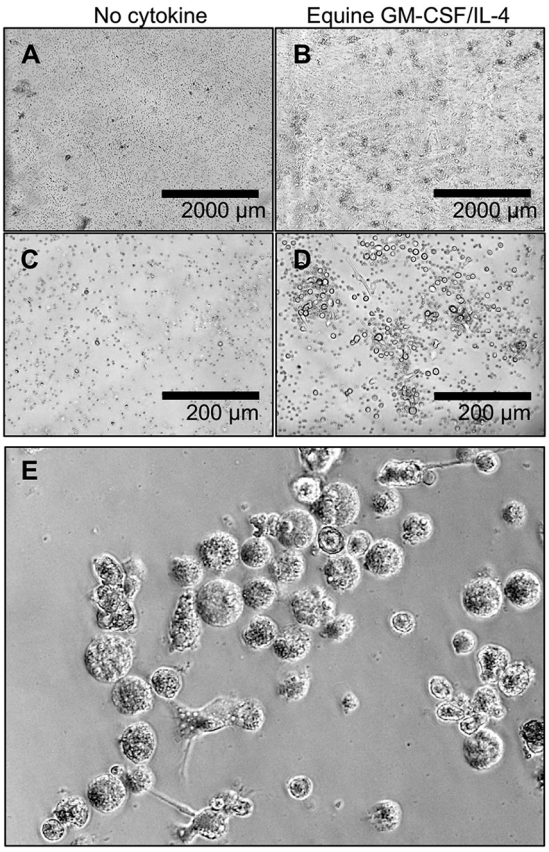

FIG 1 Egyptian rousette bat (ERB) BM cultures generate DCs in response to cytokines. BM from ERBs was cultured in bacterial petri dishes and fed either medium without cytokines (A and C) or medium supplemented with equine GM-CSF and IL-4 (B, D, and E). The addition of cytokines stimulated the outgrowth of clusters of cells after 6 days in culture that were in suspension or loosely adherent and surrounding adherent cells that resembled monocytes or macrophages. High magnification (D) shows spherical cells with DC-like morphology.

existence of a coevolved strategy where appropriate antiviral responses are elicited in combination with inhibition of destructive inflammatory responses and begins to reveal how ERBs control infection while avoiding disease and while tolerating sufficient replication for maintenance in the population.

RESULTS

Bone marrow cells differentiate into DCs when exposed to recombinant GM-CSF/IL-4. We and others have successfully generated cells that have been generally characterized as bone marrow (BM)-derived dendritic cells (BMDCs) from outbred animal species, including bats, upon exposure of BM cells to recombinant granulocyte-macrophage colony-stimulating factor (GM-CSF)/interleukin-4 (IL-4) (20–24). In an attempt to generate BMDCs from ERBs, we isolated BM cells from uninfected ERBs and cultured them in medium that contained either recombinant human, mouse, or equine GM-CSF/IL-4 or medium without cytokines. By day 6 in culture, foci of elongated cells were observed to adhere to the bacterial plates, and conspicuous outgrowth of clusters of cells in suspension was apparent only in the cultures that contained equine cytokines (Fig. 1A to D). Control cultures contained only small cells in suspension. Equine cytokines were chosen due to the similar sequence identity as bat orthologs of these cytokines (24). At days 8 to 12, high and increasing numbers of cells in suspension were observed in the cultures containing equine recombinant cytokines, and these cells had the typical appearance of DCs; the cells were circular, with an increased number of cytoplasmic projections, and were loosely clustered around sparse adherent stromal

Downloaded from http://msphere.asm.org/ on April 6, 2020 by guest

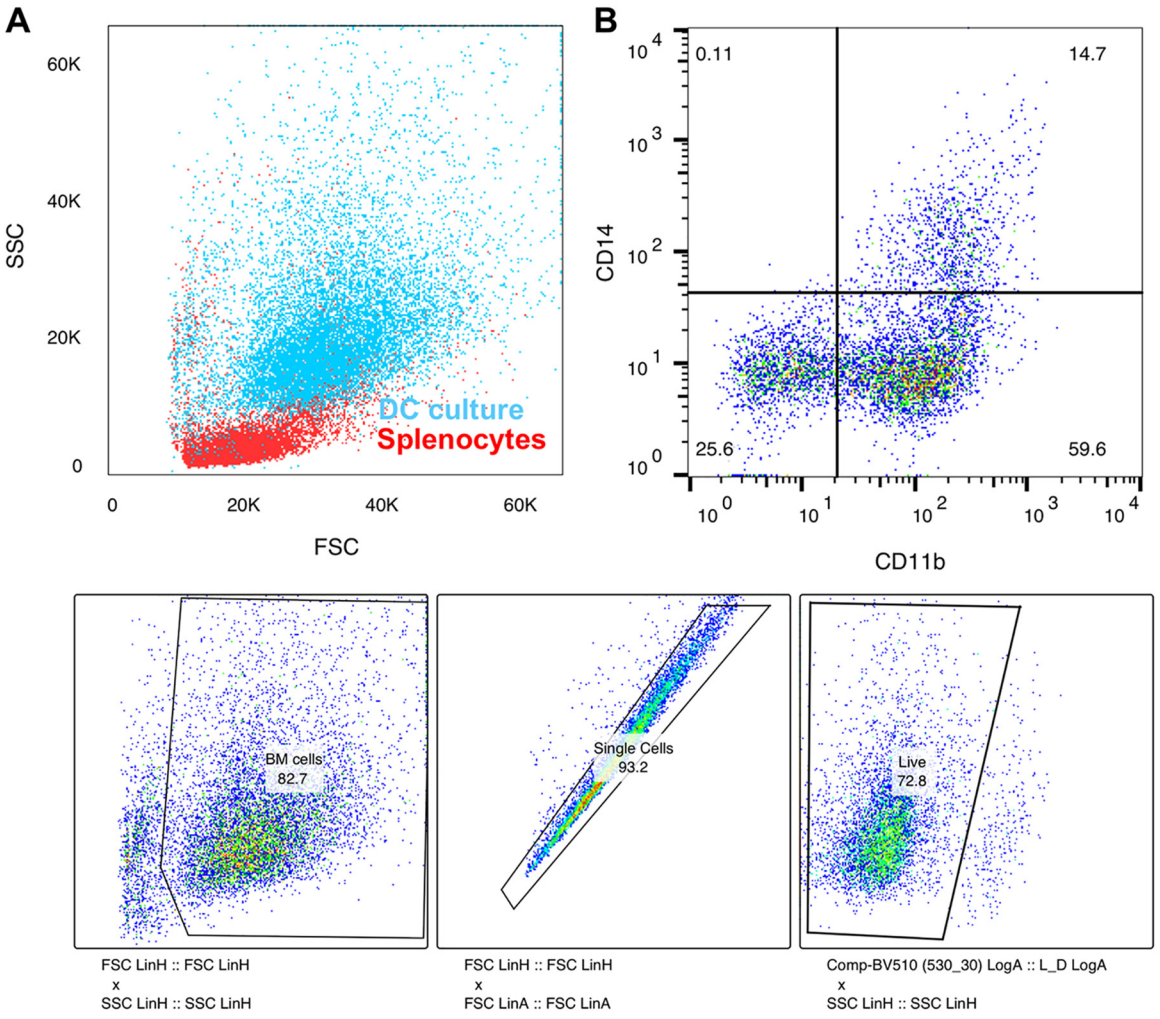

FIG 2 (A) ERB BMDCs express DC markers. BMDC cultures displayed forward-scatter (FSC) and side-scatter (SSC) properties consistent with DCs or monocytes when overlaid with total splenocytes isolated from ERBs. (B) CD11b was expressed by approximately 75% of cells, and 15% were positive for both CD11b and CD14. Virtually all cells that were $CD14^+$ also expressed CD11b.

cells (Fig. 1E). A yield of approximately 1×10^7 to 2×10^7 viable nonadherent DCs was produced 10 to 12 days after initial seeding of approximately 5×10^5 BM cells in 10-cm dishes.

To phenotypically characterize these cells, we performed flow cytometry on cells harvested 9 days after the initial culture with GM-CSF/IL-4. The forward- and side-scatter characteristics showed large cells that resembled monocyte-lineage cells when overlaid with total splenocytes from ERBs run in parallel using identical protocols and flow cytometer settings (Fig. 2A). We then examined the presence of cell surface markers indicative of BMDCs using multicolor flow cytometry (Fig. 2B). Although CD molecule expression patterns might differ between bats and humans or mice, for which they are well characterized, these molecules are highly conserved in mammals, and expression patterns on cell subsets are likely similar. The majority of cells expressed CD11b (approximately 75%), with a subset being double positive for CD11b and CD14, which is indicative of a monocyte-derived cell population undergoing differentiation toward DCs, as monocytic DCs express CD11b but are absent for CD14, and classical and intermediate monocytes are double positive in humans (25).

MARV replicates to low levels in ERB BMDCs. Since monocyte-lineage cells are major targets of filovirus infection in humans, we sought to determine whether the ERB

Downloaded from http://msphere.asm.org/ on April 6, 2020 by guest

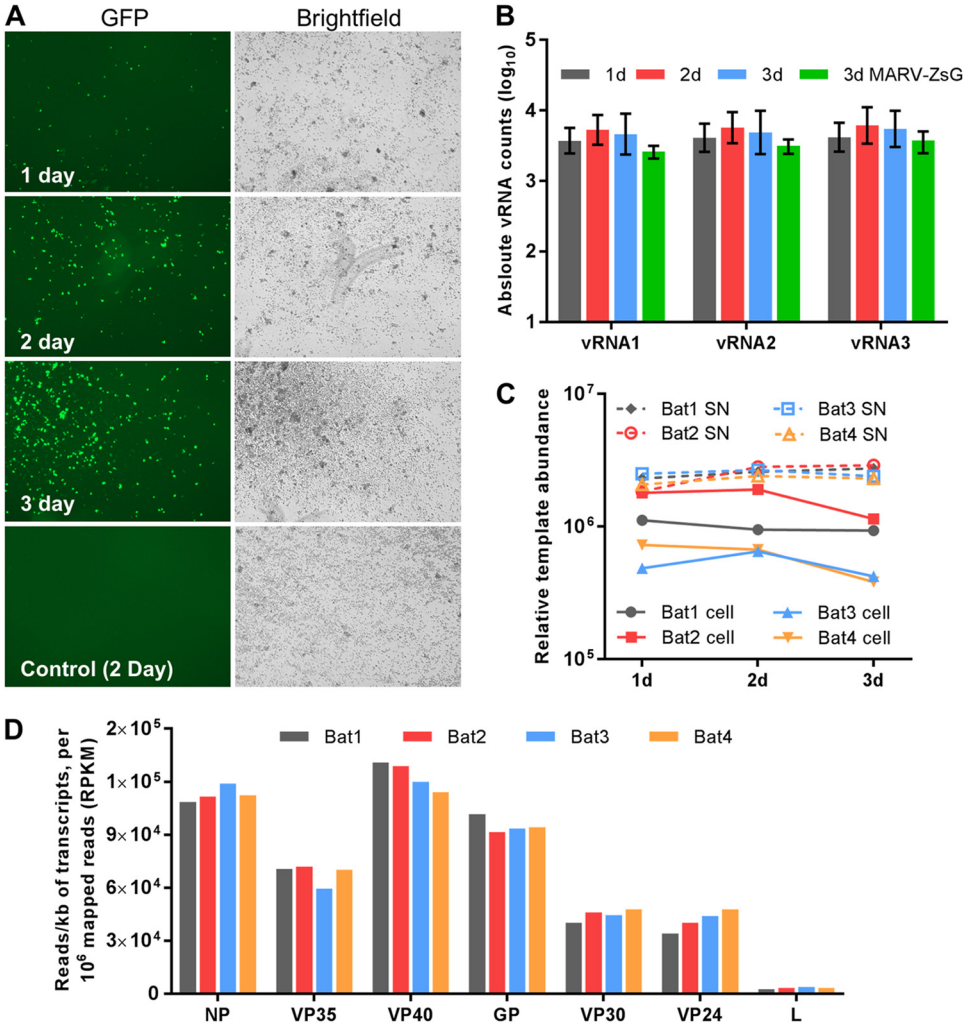

FIG 3 MARV transcription and replication in Egyptian rousette bat BMDCs. Cultures of BMDCs were infected with MARV371-ZsG (A and B) or wt-MARV371 (B to D). (A) The expression of ZsG over the course of 3 days was visualized and increased from <5% of cells infected at 1 day, when infected at an MOI of 0.5, to ~10% of cells at 3 days. GFP, green fluorescent protein. (B) Replication was assessed by measuring 3 MARV vRNA targets incorporated into the NanoString code set. Slight increases in vRNA abundance were observed between 1 and 2 days, and MARV371-ZsG had a similar level of replication at 3 days. Data are represented as the geometric means and geometric SD from 4 individual bats. (C) TaqMan assays specific for MARV were performed using total RNA from infected cells and supernatants (SN) and showed slight increases in MARV RNA between 1 and 2 days in the supernatants for all samples. (D) Transcription was measured in these samples using RNA-Seq. The transcripts were normalized using reads per kilobase of transcripts per million mapped reads to obtain the transcript abundances of all 7 MARV genes at 3 days. The transcript quantities followed an expected profile, with high levels of NP and VP40 transcripts, intermediate levels of VP30 and VP24 transcripts, and low levels of L transcripts.

BMDCs could support MARV replication. We used a recombinant bat isolate of MARV (MARV371) that expresses ZsGreen (MARV371-ZsG) to observe the kinetics of MARV371 infection in cultured ERB BMDCs. Cells were infected with MARV371-ZsG at a multiplicity of infection (MOI) of approximately 0.5, as measured on Vero E6 cells, and observed for 3 days. By 1 day, conspicuous ZsG expression was apparent in <5% of cells (Fig. 3A). The expression of ZsG increased in intensity as well as in the number of cells out to 3 days, at which time between 10 and 15% of cells showed robust ZsG protein expression. ZsG expression is indicative of viral gene translation, as ZsG is fused to NP (26) We then examined the kinetics of replication and transcription of wild-type MARV371 (wt-MARV371) in these cells. DCs were infected with wt-MARV371 at an MOI of 2, and RNA was extracted from cells and supernatants harvested at 1, 2, and 3 days. Viral RNA

Downloaded from http://msphere.asm.org/ on April 6, 2020 by guest

levels remained constant over the course of the 3 days in the cells measured using three different vRNA targets in the NanoString code set (Fig. 3B). Comparison of the viral RNAs between MARV371-ZsG- and MARV371-infected cells at 3 days showed that similar but slightly higher levels of wt-MARV371 viral RNA were present, corresponding to the higher MOI of MARV371, suggesting that MARV371-ZsG and wt-MARV371 replicate similarly (Fig. 3B). Real-time quantitative reverse transcriptase PCR (qRT-PCR) of cellular RNA and RNA from the supernatant of these cells recapitulated the NanoString results, with little change in viral RNA levels throughout the time course (Fig. 3C). To assess MARV371 transcription in BMDCs, deep sequencing (RNA-Seq) was used to measure transcripts of all 7 viral genes at 1 day. MARV371 infection resulted in an expected transcriptional gradient, with the most abundant transcripts being the earlier-transcribed genes (NP, VP40, and GP), indicating active viral transcription within these cells (Fig. 3D). Taken together, these data demonstrate low but constant levels of MARV371 replication and transcription in these BMDCs.

MARV induces the transcription of IFN-related genes but inhibits cytokines and chemokines. *In vivo*, ERBs are able to largely clear MARV by approximately 2 weeks after inoculation (8). Presumably, host innate and or adaptive immune responses play a central role in controlling and clearing these infections while preventing the immune-mediated pathology observed in humans and in animal models of disease. To determine how DCs of the natural reservoir respond to MARV infection, we examined the transcriptional host response to infection in BMDCs between 1 and 3 days following exposure to wt-MARV371 using NanoString technology and an ERB-specific gene code set comprised of 380 ERB genes (see Table S1 in the supplemental material) (27). As a control for gene expression in these cells, lipopolysaccharide (LPS) or Sendai virus (SeV) was used to stimulate the ERB BMDCs. Treatment with LPS or SeV resulted in the upregulation of several genes involved in innate immunity and DC maturation (Fig. 4A). SeV infection resulted in a greater response, with more genes being upregulated and to a greater level, as well as downregulation of several genes. Infection with MARV371 resulted in an early upregulation of a large set of genes and a strong downregulation of *CXCL2*, *IL33*, *OAS1*, *PDGFRB*, and *WNT2*. By 2 days, many of the genes that were up- or downregulated at 1 day returned to baseline, whereas other genes, such as *EIF2AK2*, *IFIT1*, *IFIT2*, *ISG15*, and *OAS3*, were upregulated beginning at this time point. By 3 days, *IFI6*, *IRF7*, *LGALS9*, and *USP18* were strongly upregulated. The mRNAs for *CCL8*, *CD80*, *IL18R1*, *LIMK1*, and *MIP-1A* were downregulated only at the 3-day time point. The mRNA for *ICAM1* was downregulated only at 2 days postinfection (dpi) (Fig. 4A). Notably, little variation was observed between the experimental replicates of 4 BMDC samples, which were derived from 4 different ERBs (Fig. 4B). Although cells derived from bat 2 showed the greatest gene regulation (up or down) in most cases, the trend of regulation was the same for all bats when genes were regulated to approximately 10-fold and oftentimes even below 10-fold.

MARV upregulates antiviral pathways and inhibits proinflammatory and maturation pathways in BMDCs. We used Ingenuity Pathway Analysis (IPA) to predict the upstream pathways, relative to those seen in humans, that result in the gene expression profile that we observed as well as the downstream pathways that are either activated, inhibited, or dysregulated. To examine if ERB BMDCs respond in a similar manner to BMDCs from other species, we examined the effect on signaling pathways upon exposure to LPS or infection by SeV. Exposure to LPS resulted in the positive upregulation of several pathways involving pattern recognition receptors (PRRs), NF-κB signaling, and DC maturation, as expected in the case of LPS stimulation of DCs (Fig. 5A). Pathways upregulated as a result of SeV infection included IFN signaling, DC maturation, and the activation of IFN regulatory factors (IRFs). Genes for pattern recognition receptors involved in recognition and neuroinflammation signaling were downregulated, whereas signaling involving innate-adaptive immune responses was dysregulated, with some genes involved in these pathways having positive effects and others having a negative effect (Fig. 5B).

Downloaded from http://msphere.asm.org/ on April 6, 2020 by guest

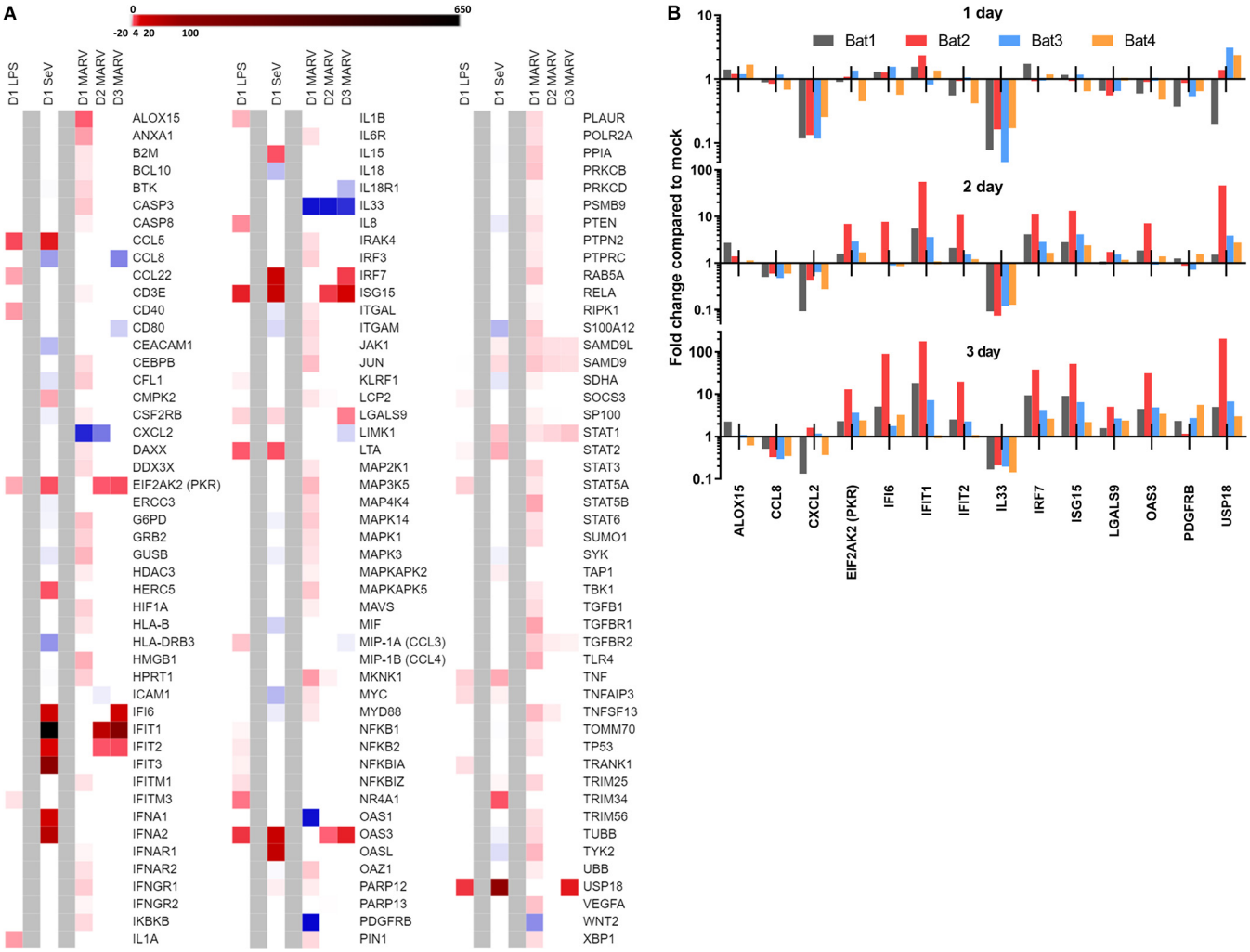

FIG 4 Host transcriptional responses to MARV in ERB BMDCs. Total RNA was extracted from 4 cultures of BMDCs infected with wt-MARV371 at an MOI of 2 and used to quantitate the expression of 380 ERB-specific genes using NanoString. Cultures treated with LPS or infected with Sendai virus (SeV) were harvested at 1 day. Significant changes in gene expression that meet the requirements of a *P* value of <0.05, >1.5-fold up- or downregulation, and >2 times the standard deviation of the uninfected controls are shown. (A) Heat map showing the genes that meet these requirements under any of the conditions (LPS, SeV, or MARV) at any time point. (B) Selected genes for visualization of the individual BMDC samples over time.

We then assessed the pathways resulting in the gene expression changes to MARV371 infection in BMDCs and found that IPA-predicted upstream regulators that are positively activated at 1 day include several genes involved in innate and adaptive immune responses (Fig. 5C). At 1 day, only the IL-10 upstream regulator was strongly inhibited. By 2 days, IFN-α and IFN-γ poly(I·C)-RNA pathways were still positively regulated; however, Toll-like receptor 3 (TLR3) and LPS pathways were inhibited. By 3 days, only the TLR3 upstream predicted pathway was inhibited. IPA was then used to determine the downstream pathways that were significantly regulated in response to MARV infection (Fig. 5D). The Th1 and Th2 activation pathways, IL-12 signaling and production, glucocorticoid receptor signaling, the IL-15 pathway, and rheumatoid arthritis pathways were all strongly and significantly dysregulated at 1 day. By 2 days, most immune-related pathways were dysregulated, with the exception of DC maturation, which was strongly downregulated. At 3 dpi, IFN signaling pathways were strongly upregulated, as was the related IRF activation by the PRR pathway; however, the NF-κB signaling pathway was downregulated. The IFN signaling pathway was activated to the highest degree at 3 days, suggesting a strong antiviral response to MARV infection. The most inhibited pathway through-

Downloaded from http://msphere.asm.org/ on April 6, 2020 by guest

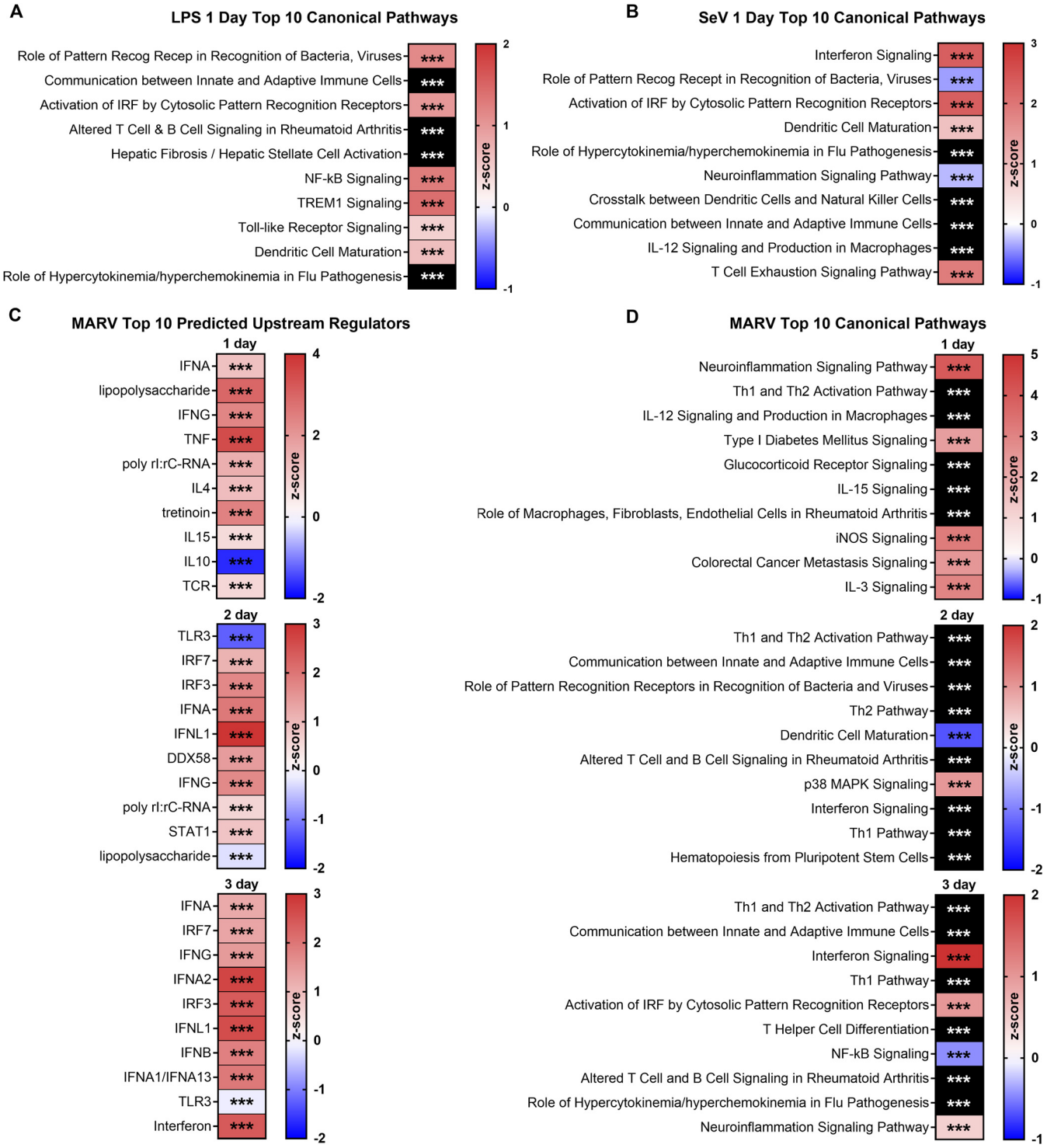

FIG 5 MARV activates antiviral responses and inhibits maturation and inflammatory responses in Egyptian rousette bat BMDCs. Ingenuity Pathway Analysis (IPA) was performed using the gene regulation data. (A and B) The top 10 pathways and their upregulation (red boxes), downregulation (blue boxes), or dysregulation (black boxes) for LPS (A) and SeV (B) at 1 day posttreatment. The Z-score indicates the strength of activation or inhibition of a pathway. (C and D) The top 10 upstream predicted regulators of the observed gene expression profiles in response to MARV371 infection at 1, 2, and 3 days postinfection (C) and the top 10 canonical downstream pathways at 1 day, 2 days, and 3 days (D). Only significant activation (red boxes), downregulation (blue boxes), and dysregulation (some genes in the predicted pathway are significantly activated, whereas others are significantly inhibited) (black boxes) are displayed. iNOS, inducible nitric oxide synthase; MAPK, mitogen-activated protein kinase.

Downloaded from http://msphere.asm.org/ on April 6, 2020 by guest

out the time course of infection was the DC maturation pathway, suggesting that MARV actively inhibits the maturation of these cells.

DISCUSSION

Little is known about how reservoirs of highly pathogenic zoonotic viruses are able to immunologically cope with infection by their respective viruses. Furthermore, several coevolved mechanisms likely exist, and each is host/virus specific. In MARV-infected ERBs, the viral load is reduced to below detectable levels within a few weeks (28). To begin to understand how MARV infects and replicates in ERBs without causing overt disease, we generated BMDCs from ERBs and assessed transcription and replication kinetics of a bat isolate of MARV, along with the host transcriptional response to MARV infection. These data provide the first insight into how ERBs immunologically respond to MARV, namely, by upregulating antiviral pathways to temper replication while simultaneously downregulating adaptive immune response modulators to prevent proinflammatory immunopathogenesis.

The methodology used here for generating BMDCs from outbred, nonlaboratory animals using GM-CSF/IL-4 has been well documented, including for bats (20, 21, 23). Despite not having specific tools for a detailed characterization the DC subtype generated by the BM of these ERBs, the observation that an outgrowth of cells morphologically similar to those previously reported and their transcriptional responses to treatment with LPS and infection with SeV strongly suggest that the majority of the cells in culture develop into bona fide DCs. This was confirmed using flow cytometry; the majority of cells expressed CD11b, and a subset of those cells expressed CD14, indicative of a monocytic cell population transitioning to monocyte-derived DCs (25).

We show that ERB BMDCs are susceptible to MARV infection and that active viral transcription is taking place out to 3 days, as evidenced by the transcriptional gradient measured by RNA-Seq and by ZsG expression of recombinant bat MARV371. Although human MDDCs infected with EBOV show infection and replication kinetics similar to what we observe here, with only a small percentage of DCs becoming infected compared to the MOI used and little replication between 1 and 3 days (29), we detected lower levels of replication between 1 and 3 days than what was previously reported for human MDDCs infected with MARV (13). These variations in responses to MARV could be due to differences in the virus isolates (human versus bat) or cell preparations (BMDCs versus MDDCs) or, more likely, due to the induction of strong cellular antiviral responses that we describe in this study, which are uniquely stimulated by MARV infection in bat DCs.

Upon examining ERB BMDC responses to infection by quantitating host transcriptional responses, two things become apparent: (i) IFN-related genes and pathways with antiviral properties are significantly upregulated, and (ii) genes and their pathways that promote DC maturation and adaptive immune responses are significantly downregulated or dysregulated. When we investigated ERB BMDC responses to infection, we found strong transcriptional induction of IFN-related antiviral responses, including the upregulation of *STAT1* by 1 day; *PKR*, *IFIT1*, *IFIT2*, *ISG15*, and *OAS3* by 2 days; and *IFI6* and *IRF7* at 3 days. This is in marked contrast to the transcriptional responses measured in human DCs infected with EBOV *in vitro*, where genes of the innate immune responses are not induced and are antagonized by VP35, with only a modest upregulation of *IFNb1* (30). IPA shows that the ERB BMDCs respond by a significant upregulation of IFN signaling, and the upstream predictors of the gene expression profile observed are primarily type I IFN and IFN-related transcription factors that are associated with antiviral responses. This unique activation might directly relate to the expansion and diversification of ERB immune genes that were recently hypothesized to be a mechanism of tolerance to viral infection by these bats (19).

While some information exists as to the transcriptional responses to EBOV in relevant cell types, there is a paucity of information for responses to MARV *in vitro*. In MARV-infected nonhuman primates (NHPs), many chemokine and cytokine genes were

Downloaded from http://msphere.asm.org/ on April 6, 2020 by guest

upregulated at early time points in peripheral blood mononuclear cells (PBMCs), in line with the model that viral proteins antagonize IFN, thereby allowing for uncontrolled viral replication and a subsequent cytokine storm (31). Although the responses in NHPs were measured in PBMCs, the early time points of gene upregulation indicate that cells possessing innate sensors of infection, such as macrophages and DCs, are responsible for gene regulation. In ERB BMDCs, cytokine and chemokine genes were either not regulated or significantly downregulated, as in the case of *CCL8*, which encodes a chemokine that recruits leukocytes to sites of infection (32). The transcription of *CCL8* was strongly upregulated throughout the course of disease in NHPs infected with MARV, starting as early as 1 dpi (31). In response to infection with EBOV, NHPs with fatal infections upregulate *CCL8* beginning at 4 dpi (33). Similar to *CCL8*, *CXCL2* encodes a chemokine that is proinflammatory (32) and is upregulated in mice that succumb to EBOV infection (34) but downregulated here in ERB BMDCs. We observe that mRNAs of DC activation and costimulatory molecules are either not induced, such as *CD40*, or downregulated, such as *CD80*. In human cells infected with either MARV or EBOV, protein levels of the costimulatory molecules CD40 and CD80 were similarly not induced (13, 29). Here, IPA showed a significant downregulation of DC maturation and NF-κB signaling, whereas several other pathways related to adaptive immune responses, such as the Th1 and Th2 pathways, and communication between innate and adaptive immune cells are significantly dysregulated.

The most strongly downregulated gene was *IL33*, which was downregulated at all time points in MARV371-infected ERB BMDCs. Mechanistically, IL-33 acts as an alarmin that is stored in the nucleus of several cell types and potentiates Th2 inflammatory and antibody responses upon release. IL-33 also promotes DC development from BM (35). IL-33 is centrally important in dengue virus infection and is strongly upregulated in mice that develop disease. The addition of recombinant exogenous IL-33 in dengue virus-infected mice resulted in severe disease with proinflammatory cytokine production and liver damage; thus, neutralization of IL-33 has been proposed as a target for therapeutics (36). The release of IL-33 is also important for responses to malaria and hepatotropic viruses, where high levels of IL-33 correlate with hepatic damage in humans (37). The downregulation of *IL33* in infected ERB BMDCs may be a coevolved response to limit proinflammatory responses. It may also relate to the observation that ERBs generate relatively weak and short-lived antibody responses to MARV infection, with IgG levels waning to undetectable levels by 3 months postinfection (8). In NHPs infected with MARV, nuclear IL-33 protein was lost in high endothelial venules and fibroblastic reticular cells of the lymph node, despite being absent for MARV antigen, suggesting that the protein is released as an alarmin and might act to promote the uncontrolled inflammatory responses that potentiate disease in NHPs (38). It will be important to assess the consequences of *IL33* downregulation in other cells and in tissues of infected ERBs, as this protein may be important for the balance that ERBs have achieved between inhibiting the production of antibodies and Th2 responses and limiting cytokine-induced pathology.

Conversely, the mRNA for Galectin-9 (LGALS9) was strongly upregulated at 3 dpi, and the Th1 and Th2 pathways were perturbed at all 3 time points by MARV infection. LGALS9 promotes and stabilizes inducible regulatory T cells (iTregs) (39). In DCs, LGALS9 is important for pathogen uptake and is indispensable for phagocytosis (40). Treg responses in the natural reservoirs of viral hemorrhagic fevers (VHFs) have been observed previously, as the rodent reservoirs of hantaviruses avoid immunopathology by the upregulation of Tregs to actively counteract inflammatory responses (41, 42).

Antagonism of the innate immune response has emerged as an important contributor to pathogenesis for many viruses, including pathogenic filoviruses. The VP35 and VP40 proteins of MARV possess several strategies to antagonize or otherwise subvert interferon-related innate immune responses upon infection of cells of certain species (14, 43). Presumably, these viruses have evolved this ability within the natural reservoir hosts, as infections of humans are thought to primarily be dead-end events. What is

Downloaded from http://msphere.asm.org/ on April 6, 2020 by guest

unknown is the specific roles that antagonism plays in the reservoir hosts and why inhibition of IFN responses is not detrimental to the host. IFN antagonism likely regulates the balance between effective innate immune responses that control virus replication and prevent inflammatory-related disease, as in the case of ERBs, and uncontrolled MARV replication that would result in immunopathogenesis, perhaps in a cell type-specific manner. In contrast to the responses in BMDCs presented here, where we see a strong upregulation of upstream and downstream IFN signaling pathways, our group recently investigated the transcriptional responses to MARV in a kidney-derived cell line from ERBs. Despite the much higher level of MARV replication in the kidney cell line than in the BMDCs, or perhaps as a result of it, almost no IFN-related antiviral gene regulation was measured, similar to what is observed in humans and disease models. The lack of IFN-related responses in ERB kidney cells was due to the interferon-antagonistic activities of VP35 (27).

The results presented here begin to elucidate how innate immune cells of coevolved hosts manage filovirus infection and show that the responses to MARV infection/replication differ between bats and dead-end hosts and even differ between cell types of the same host. Where MARV inhibits antiviral IFN-related responses in human cells universally (specialized innate immune cells and non-innate immune cells) and in non-innate immune cells in the ERB host, these antiviral responses are uniquely induced in ERB DCs. The ability of ERB DCs to overcome MARV-directed antagonism of antiviral responses is likely a coevolved and essential strategy directed toward the controlled elimination of MARV and diminished DC-mediated dissemination, while MARV simultaneously antagonizes IFN responses in nonimmune cells to a level that allows for sufficient replication for transmission and maintenance in the natural reservoir.

MATERIALS AND METHODS

Biosafety. Work with infectious agents and infected animals was conducted at the CDC (Atlanta, GA, USA) in a biological safety level 4 (BSL-4) laboratory in agreement with Select Agent protocols and practices (www.selectagents.gov). Researchers and animal care staff worked in accordance with BSL-4 level safety principles and adhered to proper infection control procedures.

Ethics statement. Work with ERBs was approved by the Institutional Animal Care and Use Committee (IACUC) of the CDC. The CDC is accredited by the Association for Assessment and Accreditation of Laboratory Animal Care International (AAALAC).

Isolation of bone marrow and generation of bone marrow-derived dendritic cells. Bone marrow (BM) was obtained from captive ERBs of Ugandan origin (28) that were euthanized for unrelated studies at the CDC. The animals were adult males. The radii and humeri were excised and then cleaned of tissue. Following the removal of the epiphyses and cutting of the radii in half, the BM was flushed out of the bones using 5 ml of cold Hanks' balanced salt solution (HBSS) and 20-gauge blunt-ended syringes and collected in a 15-ml tube containing 5 ml of ice-cold HBSS. The BM was then triturated to break up clumps, centrifuged at $350 \times g$ for 7 min, and gently resuspended in the residual HBSS after pouring off the supernatant. The cells were then enumerated and either cryopreserved in 90% fetal bovine serum (FBS)–10% dimethyl sulfoxide (DMSO) (1×10^7 to 2×10^7 cells/ml) or used directly for cultures.

For the generation of DCs, BM cells were washed in RPMI 1640 containing 10% FBS, HEPES, and antibiotics (complete RPMI medium), and approximately 2×10^6 cells were plated in 10-cm bacterial (non-tissue-culture-treated) petri dishes containing 10 ml of prewarmed complete RPMI medium or complete medium supplemented with recombinant cytokines (RPMI+C). Cytokines used were a combination of either human, mouse (both from R&D Biosystems), or equine (Kingfisher Bio) GM-CSF and IL-4 at 25 mg/ml each. After incubation for 3 days (37°C in 5% CO_2), an additional 10 ml of complete RPMI+C was added, and at 6 days, 10 ml of medium was gently pipetted off the petri dishes and replaced with fresh prewarmed complete RPMI+C. This was repeated on day 8 and every 2 days thereafter until the cells were harvested for use in experiments. Cells were harvested 1 to 2 days after conspicuous growth was observed, typically between days 10 and 12. For harvesting, the petri dishes were gently rinsed in medium to remove the nonadherent and loosely adherent cells. These cells were washed once in RPMI medium and then resuspended in complete RPMI+C for plating in 48-well tissue culture plates (5×10^5 cells) or retained in 15-ml tubes for infections prior to plating.

Infection of BMDCs. Cells that were freshly harvested and enumerated were resuspended in a minimal volume of RPMI medium and incubated with either MARV (isolate Uganda 200704852 Uganda Bat, termed MARV371) at an MOI of 2 or the bat isolate of MARV371 expressing ZsGreen (MARV371-ZsG) at an MOI of 0.5 (26) for 1 h at 37°C with 5% CO_2, with periodic gentle mixing. Cells were then washed, and 5×10^5 cells were plated in 24-well plates in complete RPMI+C. At the indicated time points, cells and supernatants were harvested and used for experiments. For Sendai virus infection, 30 hemagglutination (HA) units (MOI = 1) of the Cantell strain were added directly to the cells in 48-well plates. Cells

Downloaded from http://msphere.asm.org/ on April 6, 2020 by guest

infected with MARV-ZsG were visualized and images were captured using an Evos cell imaging system (Thermo Fisher).

Flow cytometry. DCs were harvested from bacterial petri dishes by gently rinsing and collecting the nonadherent cells and washed in Dulbecco's phosphate-buffered saline (DPBS) prior to staining for viability with Live/Dead Aqua viability dye (Invitrogen). Cells were then washed in PBS containing 2% rat serum before incubation with a custom rat anti-*Rousettus aegyptiacus* CD14-phycoerythrin (PE) antibody and an anti-human/mouse CD11b-allophycocyanin (APC)/Fire 750 antibody (BioLegend). The cells were then washed and fixed in Cytofix/Cytoperm (BD Biosciences) overnight and washed again in PBS containing 2% rat serum, flow cytometry was performed using a Stratedigm custom cytometer (Stratedigm, Inc.), and data were analyzed using FlowJo software, version 10 (TreeStar).

RNA isolation and quantitative reverse transcriptase PCR. DCs were harvested using MagMAX RNA lysis/binding solution concentrate (Thermo Fisher Scientific), and RNA was extracted by magnetic bead purification using the MagMAX-96 DNA/RNA pathogen kit run in a MagMAX Express-96 magnetic particle processor (Thermo Fisher Scientific). qRT-PCR was conducted using the SuperScript III Platinum one-step qRT-PCR kit (Thermo Fisher), using TaqMan-based probes against MARV VP40.

Gene expression measured by NanoString. A custom NanoString nCounter ERB-specific code set targeting 380 ERB and 10 MARV genes was designed by NanoString Technologies using the Raegyp2.0 genome assembly (RefSeq accession number GCF_001466805.2) and NCBI *R. aegyptiacus* annotation release 100, expanded from a previous code set that consisted of 221 genes (see Table S1 in the supplemental material) (27). Hybridization reactions were performed according to the manufacturer's instructions, as previously described (27). Briefly, hybridization buffer was mixed with the reporter code set reagent, aliquoted into PCR tubes, and then mixed with total RNA from DCs and finally with the Capture ProbeSet reagent. Samples were pulse spun and incubated for 24 h at 65°C. Sample sets were then loaded onto an nCounter cartridge and run in an nCounter Sprint profiler for count data collection.

nCounter transcriptomic analysis. nCounter data were processed using nSolver 4.0 software (NanoString). After quality control of RCC files, raw counts across all samples were normalized, without background subtraction or thresholding, to the geometric mean counts of synthetic positive controls included in hybridization reactions. The top five most stable genes in each tissue data set were selected as reference genes using the geNorm algorithm within the nCounter Advanced Analysis (nCAA) module (version 2.0.115). For each sample, normalization was performed by dividing counts for each gene by the geometric mean of the five reference genes. nCAA was used to calculate differential gene expression (DGE) of each data set. Significance, relevance, and count threshold criteria used for DGE analysis at each time point were set to a minimum of a $\pm$1.5-fold change (FC), a Benjamini-Yekutieli-adjusted P value of $<$0.05 (44), and an above-background count threshold of 2 times the standard deviation (SD) of the mean counts of all synthetic negative controls across all samples. In order to be considered a bona fide differentially expressed gene (DEG) in any given data set, all three criteria were required for at least one time point value.

RNA-Seq data collection and analysis. RNA was evaluated for quality on the Agilent 2200 TapeStation. Libraries were generated on the Sciclone G3 liquid-handling robot (PerkinElmer) using the TruSeq stranded total RNA library prep kit (Illumina). Library quality was assessed on the TapeStation and quantitative PCR (qPCR) quantitated using the Kapa complete (universal) qPCR kit (Kapa Biosystems) for Illumina. Libraries were diluted to 12 pM, cluster generation was performed on the Illumina cBot, and sequencing was performed on the HiSeq 2500 system using the paired-end 2- by 125-bp, dual-index format. Raw reads were first verified by FastQC and then trimmed for low-quality reads/adapters and filtered using Trimmomatic-0.33. Analyses of next-generation sequencing (NGS) data, including read mapping and variant detection, were done using CLC Genomics Workbench 9.1.

Pathway analysis. Ingenuity Pathway Analysis (IPA; Qiagen Bioinformatics) was used to determine significantly enriched pathways and upstream regulators for each tissue data set.

SUPPLEMENTAL MATERIAL

Supplemental material for this article may be found at https://doi.org/10.1128/mSphere.00728-19.

TABLE S1, PDF file, 0.1 MB.

ACKNOWLEDGMENTS

The findings and conclusions in this report are those of the authors and do not necessarily represent the official position of the Centers for Disease Control and Prevention.

We declare that the research was conducted in the absence of any commercial or financial relationships that could be construed as a potential conflict of interest.

This study was funded in part by DTRA grant HDTRA-14-1-0016.

REFERENCES

1. Goldstein T, Anthony SJ, Gbakima A, Bird BH, Bangura J, Tremeau-Bravard A, Belaganahalli MN, Wells HL, Dhanota JK, Liang E, Grodus M, Jangra RK, DeJesus VA, Lasso G, Smith BR, Jambai A, Kamara BO, Kamara S, Bangura W, Monagin C, Shapira S, Johnson CK, Saylors K, Rubin EM, Chandran K, Lipkin WI, Mazet JAK. 2018. The discovery of Bombali virus adds further support for bats as hosts of ebolavi-

Downloaded from http://msphere.asm.org/ on April 6, 2020 by guest

ruses. Nat Microbiol 3:1084–1089. https://doi.org/10.1038/s41564-018-0227-2.
2. Yang X-L, Tan CW, Anderson DE, Jiang R-D, Li B, Zhang W, Zhu Y, Lim XF, Zhou P, Liu X-L, Guan W, Zhang L, Li S-Y, Zhang Y-Z, Wang L-F, Shi Z-L. 2019. Characterization of a filovirus (Měnglà virus) from Rousettus bats in China. Nat Microbiol 4:390–395. https://doi.org/10.1038/s41564-018-0328-y.
3. Towner JS, Amman BR, Sealy TK, Carroll SAR, Comer JA, Kemp A, Swanepoel R, Paddock CD, Balinandi S, Khristova ML, Formenty PBH, Albarino CG, Miller DM, Reed ZD, Kayiwa JT, Mills JN, Cannon DL, Greer PW, Byaruhanga E, Farnon EC, Atimnedi P, Okware S, Katongole-Mbidde E, Downing R, Tappero JW, Zaki SR, Ksiazek TG, Nichol ST, Rollin PE. 2009. Isolation of genetically diverse Marburg viruses from Egyptian fruit bats. PLoS Pathog 5:e1000536. https://doi.org/10.1371/journal.ppat.1000536.
4. Negredo A, Palacios G, Vázquez-Morón S, González F, Dopazo H, Molero F, Juste J, Quetglas J, Savji N, de la Cruz Martínez M, Herrera JE, Pizarro M, Hutchison SK, Echevarría JE, Lipkin WI, Tenorio A. 2011. Discovery of an ebolavirus-like filovirus in Europe. PLoS Pathog 7:e1002304. https://doi.org/10.1371/journal.ppat.1002304.
5. Schuh AJ, Amman BR, Towner JS. 2017. Filoviruses and bats. Microbiol Aust 38:12–16. https://doi.org/10.1071/MA17005.
6. Coltart CEM, Lindsey B, Ghinai I, Johnson AM, Heymann DL. 2017. The Ebola outbreak, 2013–2016: old lessons for new epidemics. Philos Trans R Soc Lond B Biol Sci 372:20160297. https://doi.org/10.1098/rstb.2016.0297.
7. Pigott DM, Golding N, Mylne A, Huang Z, Weiss DJ, Brady OJ, Kraemer MUG, Hay SI. 2015. Mapping the zoonotic niche of Marburg virus disease in Africa. Trans R Soc Trop Med Hyg 109:366–378. https://doi.org/10.1093/trstmh/trv024.
8. Schuh AJ, Amman BR, Jones MEB, Sealy TK, Uebelhoer LS, Spengler JR, Martin BE, Coleman-McCray JAD, Nichol ST, Towner JS. 2017. Modelling filovirus maintenance in nature by experimental transmission of Marburg virus between Egyptian rousette bats. Nat Commun 8:14446. https://doi.org/10.1038/ncomms14446.
9. Prescott JB, Marzi A, Safronetz D, Robertson SJ, Feldmann H, Best SM. 2017. Immunobiology of Ebola and Lassa virus infections. Nat Rev Immunol 17:195–207. https://doi.org/10.1038/nri.2016.138.
10. Rougeron V, Feldmann H, Grard G, Becker S, Leroy EM. 2015. Ebola and Marburg haemorrhagic fever. J Clin Virol 64:111–119. https://doi.org/10.1016/j.jcv.2015.01.014.
11. Liu YJ. 2001. Dendritic cell subsets and lineages, and their functions in innate and adaptive immunity. Cell 106:259–262. https://doi.org/10.1016/S0092-8674(01)00456-1.
12. Banchereau J, Briere F, Caux C, Davoust J, Lebecque S, Liu Y-J, Pulendran B, Palucka K. 2000. Immunobiology of dendritic cells. Annu Rev Immunol 18:767–811. https://doi.org/10.1146/annurev.immunol.18.1.767.
13. Bosio CM, Aman MJ, Grogan C, Hogan R, Ruthel G, Negley D, Mohamadzadeh M, Bavari S, Schmaljohn A. 2003. Ebola and Marburg viruses replicate in monocyte-derived dendritic cells without inducing the production of cytokines and full maturation. J Infect Dis 188:1630–1638. https://doi.org/10.1086/379199.
14. Ramanan P, Shabman RS, Brown CS, Amarasinghe GK, Basler CF, Leung DW. 2011. Filoviral immune evasion mechanisms. Viruses 3:1634–1649. https://doi.org/10.3390/v3091634.
15. Feldmann H, Bugany H, Mahner F, Klenk HD, Drenckhahn D, Schnittler HJ. 1996. Filovirus-induced endothelial leakage triggered by infected monocytes/macrophages. J Virol 70:2208–2214.
16. Stroher U, West E, Bugany H, Klenk H-D, Schnittler H-J, Feldmann H. 2001. Infection and activation of monocytes by Marburg and Ebola viruses. J Virol 75:11025–11033. https://doi.org/10.1128/JVI.75.22.11025-11033.2001.
17. Geisbert TW, Hensley LE, Larsen T, Young HA, Reed DS, Geisbert JB, Scott DP, Kagan E, Jahrling PB, Davis KJ. 2003. Pathogenesis of Ebola hemorrhagic fever in cynomolgus macaques: evidence that dendritic cells are early and sustained targets of infection. Am J Pathol 163:2347–2370. https://doi.org/10.1016/S0002-9440(10)63591-2.
18. Jones M, Amman B, Sealy T, Uebelhoer L, Schuh A, Flietstra T, Bird B, Coleman-McCray J, Zaki S, Nichol S, Towner J. 2019. Clinical, histopathologic, and immunohistochemical characterization of experimental Marburg virus infection in a natural reservoir host, the Egyptian rousette bat (Rousettus aegyptiacus). Viruses 11:E214. https://doi.org/10.3390/v11030214.
19. Pavlovich SS, Lovett SP, Koroleva G, Guito JC, Arnold CE, Nagle ER, Kulcsar K, Lee A, Thibaud-Nissen F, Hume AJ, Mühlberger E, Uebelhoer LS, Towner JS, Rabadan R, Sanchez-Lockhart M, Kepler TB, Palacios G. 2018. The Egyptian rousette genome reveals unexpected features of bat antiviral immunity. Cell 173:1098–1110. https://doi.org/10.1016/j.cell.2018.03.070.
20. Davenport BJ, Willis DG, Prescott J, Farrell RM, Coons TA, Schountz T. 2004. Generation of competent bone marrow-derived antigen presenting cells from the deer mouse (Peromyscus maniculatus). BMC Immunol 5:23. https://doi.org/10.1186/1471-2172-5-23.
21. Zhou P, Chionh YT, Irac SE, Ahn M, Jia Ng JH, Fossum E, Bogen B, Ginhoux F, Irving AT, Dutertre CA, Wang LF. 2016. Unlocking bat immunology: establishment of Pteropus alecto bone marrow-derived dendritic cells and macrophages. Sci Rep 6:38597. https://doi.org/10.1038/srep38597.
22. Wu Z, Rothwell L, Young JR, Kaufman J, Butter C, Kaiser P. 2010. Generation and characterization of chicken bone marrow-derived dendritic cells. Immunology 129:133–145. https://doi.org/10.1111/j.1365-2567.2009.03129.x.
23. Cody V, Shen H, Shlyankevich M, Tigelaar RE, Brandsma JL, Hanlon DJ. 2005. Generation of dendritic cells from rabbit bone marrow mononuclear cell cultures supplemented with hGM-CSF and hIL-4. Vet Immunol Immunopathol 103:163–172. https://doi.org/10.1016/j.vetimm.2004.08.022.
24. Schountz T. 2014. Immunology of bats and their viruses: challenges and opportunities. Viruses 6:4880–4901. https://doi.org/10.3390/v6124880.
25. Gustafson MP, Lin Y, Maas ML, Van Keulen VP, Johnston PB, Peikert T, Gastineau DA, Dietz AB. 2015. A method for identification and analysis of non-overlapping myeloid immunophenotypes in humans. PLoS One 10:e0121546. https://doi.org/10.1371/journal.pone.0121546.
26. Albariño CG, Wiggleton Guerrero L, Chakrabarti AK, Nichol ST. 2018. Transcriptional analysis of viral mRNAs reveals common transcription patterns in cells infected by five different filoviruses. PLoS One 13:e0201827. https://doi.org/10.1371/journal.pone.0201827.
27. Arnold CE, Guito JC, Altamura LA, Lovett SP, Nagle ER, Palacios GF, Sanchez-Lockhart M, Towner JS. 2018. Transcriptomics reveal antiviral gene induction in the Egyptian rousette bat is antagonized in vitro by Marburg virus Infection. Viruses 10:E607. https://doi.org/10.3390/v10110607.
28. Amman BR, Jones MEB, Sealy TK, Uebelhoer LS, Schuh AJ, Bird BH, Coleman-McCray JD, Martin BE, Nichol ST, Towner JS. 2015. Oral shedding of Marburg virus in experimentally infected Egyptian fruit bats (*Rousettus aegyptiacus*). J Wildl Dis 51:113–124. https://doi.org/10.7589/2014-08-198.
29. Lubaki NM, Ilinykh P, Pietzsch C, Tigabu B, Freiberg AN, Koup RA, Bukreyev A. 2013. The lack of maturation of Ebola virus-infected dendritic cells results from the cooperative effect of at least two viral domains. J Virol 87:7471–7485. https://doi.org/10.1128/JVI.03316-12.
30. Ilinykh PA, Lubaki NM, Widen SG, Renn LA, Theisen TC, Rabin RL, Wood TG, Bukreyev A. 2015. Different temporal effects of Ebola virus VP35 and VP24 proteins on global gene expression in human dendritic cells. J Virol 89:7567–7583. https://doi.org/10.1128/JVI.00924-15.
31. Connor JH, Yen J, Caballero IS, Garamszegi S, Malhotra S, Lin K, Hensley L, Goff AJ. 2015. Transcriptional profiling of the immune response to Marburg virus infection. J Virol 89:9865–9874. https://doi.org/10.1128/JVI.01142-15.
32. Zlotnik A, Yoshie O, Nomiyama H. 2006. The chemokine and chemokine receptor superfamilies and their molecular evolution. Genome Biol 7:243. https://doi.org/10.1186/gb-2006-7-12-243.
33. Speranza E, Connor JH. 2017. Host transcriptional response to Ebola virus infection. Vaccines 5:E30. https://doi.org/10.3390/vaccines5030030.
34. Cilloniz C, Ebihara H, Ni C, Neumann G, Korth MJ, Kelly SM, Kawaoka Y, Feldmann H, Katze MG. 2011. Functional genomics reveals the induction of inflammatory response and metalloproteinase gene expression during lethal Ebola virus infection. J Virol 85:9060–9068. https://doi.org/10.1128/JVI.00659-11.
35. Mayuzumi N, Matsushima H, Takashima A. 2009. IL-33 promotes DC development in BM culture by triggering GM-CSF production. Eur J Immunol 39:3331–3342. https://doi.org/10.1002/eji.200939472.
36. Marques RE, Besnard A-G, Maillet I, Fagundes CT, Souza DG, Ryffel B, Teixeira MM, Liew FY, Guabiraba R. 2018. Interleukin-33 contributes to disease severity in *Dengue virus* infection in mice. Immunology 155:477–490. https://doi.org/10.1111/imm.12988.
37. Wang J, Zhao P, Guo H, Sun X, Jiang Z, Xu L, Feng J, Niu J, Jiang Y. 2012. Serum IL-33 levels are associated with liver damage in patients with chronic hepatitis C. Mediators Inflamm 2012:819636. https://doi.org/10.1155/2012/819636.
38. Alves DA, Glynn AR, Steele KE, Lackemeyer MG, Garza NL, Buck JG, Mech

Downloaded from http://msphere.asm.org/ on April 6, 2020 by guest

C, Reed DS. 2010. Aerosol exposure to the Angola strain of Marburg virus causes lethal viral hemorrhagic fever in cynomolgus macaques. Vet Pathol 47:831–851. https://doi.org/10.1177/0300985810378597.
39. Wu C, Thalhamer T, Franca RF, Xiao S, Wang C, Hotta C, Zhu C, Hirashima M, Anderson AC, Kuchroo VK. 2014. Galectin-9-CD44 interaction enhances stability and function of adaptive regulatory T cells. Immunity 41:270–282. https://doi.org/10.1016/j.immuni.2014.06.011.
40. Cano LQ, Tagit O, van Duffelen A, Dieltjes S, Buschow SI, Niki T, Hirashima M, Joosten B, van den Dries K, Cambi A, Figdor CG, van Spriel AB. 2019. Intracellular Galectin-9 controls dendritic cell function by maintaining plasma membrane rigidity. bioRxiv https://doi.org/10.1101/739797.
41. Easterbrook JD, Zink MC, Klein SL. 2007. Regulatory T cells enhance persistence of the zoonotic pathogen Seoul virus in its reservoir host. Proc Natl Acad Sci U S A 104:15502–15507. https://doi.org/10.1073/pnas.0707453104.
42. Schountz T, Prescott J, Cogswell AC, Oko L, Mirowsky-Garcia K, Galvez AP, Hjelle B. 2007. Regulatory T cell-like responses in deer mice persistently infected with Sin Nombre virus. Proc Natl Acad Sci U S A 104:15496–15501. https://doi.org/10.1073/pnas.0707454104.
43. Basler CF. 2015. Innate immune evasion by filoviruses. Virology 479–480:122–130. https://doi.org/10.1016/j.virol.2015.03.030.
44. Benjamini Y, Yekutieli D. 2001. The control of the false discovery rate in multiple testing under dependency. Ann Stat 29:1165–1188. https://www.jstor.org/stable/2674075.

Downloaded from http://msphere.asm.org/ on April 6, 2020 by guest